Xia, Yunlong and Liang, Yanchun and Kongstad, Ole and Liao, Qiuming and Holm, Magnus and Olsson, Bertil and Yuan, Shiwen

"T_{peak}-T_{end} Interval as an Index of Global Dispersion of Ventricular Repolarization: Evaluations Using Monophasic Action Potential Mapping of the Epi- and Endocardium in Swine"

Title with different words from the published article:
"In vivo validation of the coincidence of the peak and end of the T wave with full repolarization of the epicardium and endocardium in swine."

Heart Rhythm. 2005 Feb;2(2):162-9.

Publisher: Elsevier.

Alternative location: http://dx.doi.org/10.1016/j.hrthm.2004.11.011

T_{peak}-T_{end} Interval as an Index of Global Dispersion of Ventricular Repolarization: Evaluations Using Monophasic Action Potential Mapping of the Epi- and Endocardium in Swine

Yunlong Xia, M.D., Yanchun Liang, M.D., Ph.D., Ole Kongstad, M.D., *Magnus Holm, M.S., Ph.D., Bertil Olsson, M.D., Ph.D., Shiwen Yuan, M.D., Ph.D.

Department of Cardiology, University Hospital, Lund, Sweden, and *Biosense Webster/ Johnson & Johnson Inc., Waterloo, Belgium.

Short Title: T_{peak}-T_{end} Interval: An Index of Global Dispersion of Ventricular Repolarization

This study was supported by funding from the Swedish Heart-Lung Foundation, Lund University Hospital donation funds, the Franke and Margaretha Bergqvist Foundation, and Biosense Webster/Johnson & Johnson Inc.

Correspondence to:

Shiwen Yuan, M.D., Ph.D.

Department of Cardiology

University Hospital

SE-221 85 Lund, Sweden.

Tel: +46–46–173648

Fax: +46–46–157857

E-mail: Shiwen.Yuan@kard.lu.se

Abstract

The ECG interval from the peak to the end of the T wave (T_{peak}-T_{end}) has been used as an index of transmural dispersion of ventricular repolarization (DVR). The correlation between the T_{peak}-T_{end} interval and the global DVR, however, has not been well-evaluated. **Methods:** Monophasic action potentials (MAPs) were recorded from 51±10 epicardial and 64±9 endocardial sites in the left ventricles of 10 pigs, and from 41±4 epicardial and 53±2 endocardial sites in the right ventricles of 2 of the 10 pigs using the CARTO mapping system. The end of repolarization times over the epi- and endocardium were measured, and the end of repolarization dispersions over the epicardium (DVR-epi), over the endocardium (DVR-endo) and over both (DVR-total) were calculated. The QT_{peak}, QT_{end} and T_{peak}-T_{end} intervals as well as the QT_{peak} and QT_{end} dispersions were obtained from the simultaneously recorded 12-lead ECG. **Results:** The maximal T_{peak}-T_{end} intervals (57±7 ms) were consistent with the DVR-total (58±11 ms, $p > 0.05$), and significantly correlated with the DVR-total ($r = 0.64$, $p < 0.05$). However, the mean T_{peak}-T_{end} intervals (44±5 ms), and T_{peak}-T_{end} intervals from lead II (41±6 ms) and V_5 (43±5 ms) were all significantly smaller than and poorly correlated with the DVR-total, as were the QT_{peak} and QT_{end} dispersions (15±2 ms vs. 21±4 ms). **Conclusion:** The maximal T_{peak}-T_{end} interval may be used as a noninvasive estimate for the global DVR, but not the QT_{peak} and QT_{end} dispersions, nor the mean T_{peak}-T_{end} interval and that from a single lead.

Key words: T_{peak}-T_{end} interval, monophasic action potential, global dispersion of ventricular repolarization

Introduction

An increased dispersion of ventricular repolarization (DVR) was found to be associated with increased propensity for ventricular arrhythmias, and was therefore considered an important arrhythmogenic mechanism (1, 2). Non-invasive body surface recordings have been used to define indices thought to reflect this electrophysiological substrate (3-5). However, the reliability of body surface measurements, such as recovery time dispersion and QT dispersion, has been controversial (6-8). Recently, Antzelevitch and Yan et al. demonstrated that the dispersion of repolarization may result from differences in action potential duration among cells originating from different myocardial layers, and suggested a new simple non-invasive ECG marker, T_{peak}-T_{end} interval, to represent transmural dispersion (9, 10). However, *in vivo* verifications of the theory are still lacking and the results of previous clinical studies using this index for evaluation of transmural ventricular repolarization have been inconsistent (11-13).

Monophasic activation potential (MAP) has generally been accepted as the method of choice for evaluating ventricular repolarization (14, 15). We have earlier combined the MAP recording and the electroanatomic mapping techniques (CARTO, Biosense Webster, Waterloo, Belgium) in evaluating the global ventricular repolarization (16-18). In this study, we attempted to evaluate the correlation between global DVR and the T_{peak}-T_{end} interval using MAP mapping over both the epicardium and endocardium and the 12-lead ECG in swine.

Materials and Methods

Subjects

Ten healthy pigs, 47-53 kg, were premedicated with pancuronium bromide (0.1 mg/kg), thiopental (5 mg/kg) and atropine (0.015 mg/kg). Anesthesia was maintained with an infusion of 10 ml/hour of a mixture of 1 mg fentanyl and 20 mg pancuronium bromide. Intubation and artificial ventilation of the pigs were performed during the study. Volume-controlled ventilation of 8 L/min, 20 breaths/min, a positive end-expiration pressure of 5 cm H_2O, and FiO_2 of 0.5 was used. Thoracotomy and pericardectomy were then performed to expose the heart. The study was approved by the local ethics committee and the electrophysiological procedures were in accordance with the local institutional guidelines.

The CARTO system

The system has been described in detail previously (19). In brief, the torso of the subject is covered by three magnetic fields of different frequencies. A location reference (Ref-Star, Biosense Webster) is fixed on the back of the subject, while a mapping catheter (Navi-Star, Biosense Webster) navigates within the cardiac chambers or on the surface of the heart. The magnetic sensors equipped in the tip of the mapping catheter and the location reference continuously compare the intensities of the three magnetic fields, ensuring that the location of the mapping catheter can be accurately determined and displayed in real time. Three-dimensional maps of endocardial or epicardial activation can be constructed from accurately localized electrograms recorded using the mapping catheter. The accuracy of spatial localization has been verified to be 0.7 mm *in vivo* (19).

MAP recording

Both endocardial and epicardial mapping were performed after thoracotomy and pericardectomy. In 2 pigs, both the right and left ventricles were mapped, and in the remaining 8 pigs only the left ventricle were mapped. A modified-tip, 7F Navi-Star catheter (Biosense Webster) was used, which has a contact ball of 0.5 mm length and 1 mm diameter at the end of the tip electrode (20). For endocardial mapping, the catheter was introduced into the left ventricle via the right femoral artery and into the right ventricle via the right femoral vein, whereas for epicardial mapping the catheter was mounted on an elastic handle of an epicardial-mapping probe (EP Technologies, Sunnyvale, CA). Two saline lines were hung over the left and right ventricles with warm saline drip to keep the myocardial temperature constant and to facilitate electrical contact of electrodes with the epicardium. A thermometer (myocardial needle temperature probe) was inserted into the myocardium of the right ventricular out-flow tract for monitoring of myocardial temperature during the whole experiment. The temperature and speed of the saline drip were adjusted if necessary.

MAP signals were recorded between the 4-mm length tip electrode (exploring electrode) and the 2-mm length ring electrode 1 mm proximal to the tip (indifferent electrode) at a filter bandwidth of 0.05 to 400 Hz. A unipolar electrogram from the indifferent electrode was also recorded at a filter bandwidth of 0.5 to 120 Hz. When the amplitude and morphology of the MAP in the real-time monitor window of the CARTO system appeared to be satisfactory (14), it was captured in a sampling window for further inspection. The accepted signals were stored simultaneously at a sampling frequency of 1 kHz. Care was taken to place the mapping catheter perpendicularly against the endo-/epicardium and to avoid “ST segment” elevation, i. e. >20% amplitude of the ventricular deflection, on the unipolar electrogram from the

indifferent electrode. At least one MAP was recorded in an area of 2 cm^2 during the epicardial and endocardial mapping (Fig. 1). To avoid the influence of variations in heart rate, the MAP mapping was performed during constant pacing at the high lateral right atrium at 130 beats/min.

MAP analysis

MAP analysis was performed off-line by an independent investigator using the double annotation feature of the CARTO system. The first annotation was set at the maximum slope of the MAP upstroke, representing local activation. The second was set at the intersection between the baseline and the tangent to the steepest slope on phase 3 of the MAP, representing local end of repolarization (EOR). The two annotation lines were both manually set and carefully checked with display time scales of 200 mm/s and 100 mm/s, respectively.

The activation time was defined as the time interval from the earliest recorded ventricular activation to the local activation, the EOR time as that from the earliest ventricular activation to the local EOR, and the MAP duration as that from the local activation to the local EOR. At each site these three values were obtained, taking the peak of an upright QRS complex on the surface ECG as time reference. Based on these values, three-dimensional maps of the EOR were constructed.

The minimal and maximal EOR times of the epi-/endocardium were calculated from the values obtained. The epicardial DVR (DVR-epi) was defined as the difference between the maximal and minimal EOR times over the epicardium, endocardial DVR (DVR-endo) as that between the maximal and minimal EOR times over the endocardium, and the total DVR (DVR-total) as that between the maximal and the minimal EOR times of all the recordings.

Recording of the surface ECG and measurement of the QT dispersion

Using the CARTO system, 12-lead ECG was simultaneously recorded with the electrodes being placed referencing to the electrode placement in humans. All ECGs were recorded after the thoracotomy.

The start of the QRS complex, the peak and the end of the T wave were identified separately from each of the 12 leads (Fig. 2). The earliest onset of the QRS among the 12 leads was used as the starting point for all the QT interval measurements. The peak of the T wave was defined as the time point where the T wave had the maximal amplitude. The end of the T wave was defined using the slope method, i.e. the intersection of a line tangential to the point of maximum slope of the terminal T wave with isoelectric level defined by the T-P segment. Thus, the QT_{peak}, QT_{end} and T_{peak}-T_{end} interval could be obtained from each lead. The measurement was carefully checked at sweep speeds of 50 mm/s. Leads with high noise levels, flat or distorted T waves that made the identification of T_{peak} and/or T_{end} impossible were discarded from the analysis. From the 12-lead ECG, the QT_{peak}, QT_{end} and T_{peak}-T_{end} intervals were measured manually three times at the beginning, middle and end of the MAP mapping procedure using an on-screen electronic calliper. Each time, the above parameters were measured from 2 consecutive beats and the mean was obtained. The mean values of the above mentioned 3 measurements were again averaged and the mean was used for final analysis.

In each pig, QT_{peak} dispersion was defined as the difference between the maximum and minimum of QT_{peak} intervals, and QT_{end} dispersion was defined as that between the maximum and minimum of QT_{end} intervals. Due to the variation of the peak and end of the T wave, T_{peak}-T_{end} intervals were calculated as maximal, minimal

and mean values in the 12 leads, which was from the earliest T_{peak} to the latest T_{end}, from the latest T_{peak} to the earliest T_{end}, and the average of all the T_{peak}-T_{end} intervals of the 12 leads, respectively.

Statistical analysis

All data are presented as mean ± 1 standard deviation. A *P* value < 0.05 was considered statistically significant.

Paired, two-tail Student's t-test was performed between the DVR-epi/endo and DVR-total. In addition, the QT_{peak} dispersion, QT_{end} dispersion and T_{peak}-T_{end} intervals were compared with the DVR-total, respectively. The correlation analyses were also used to study the relationship between the DVR parameters and the relevant ECG repolarization variables.

Results

General data

MAPs were recorded from 51±10 epicardial sites and 64±9 endocardial sites in the left ventricles of all 10 pigs (Fig. 2), and from 41±4 epicardial sites and 53±2 endocardial sites in the right ventricles of 2 of the 10 pigs. Based on these data, 12 sets of endocardial and epicardial maps of repolarization sequence were constructed. The MAP plateau amplitude was 13.6±5.0 mV for the epicardial MAPs and 13.6±5.6 mV for the endocardial MAPs of the left ventricles, and 12.8±4.6 mV for the epicardial MAPs and 13.0±5.0 mV for the endocardial MAPs of the right ventricles. The baseline disturbance was less than 10% of the plateau amplitude in 80% and less than 15% of the plateau amplitude in all the 591 epi- and 746 endocardial recordings.

Twelve-lead ECG was recorded after the thoracotomy and pericardectomy. No motion artefact from the heartbeat was observed in ECG during the MAP mapping procedure. The baseline appeared stable without 50-Hz disturbances. During QT intervals measurement, 1±1 leads were discarded due to the flat and/or distorted T waves. No U wave was documented in any of the 10 pigs.

When measuring the EOR times and QT intervals, the onset of the earliest QRS was used as the earliest recorded ventricular activation in all 10 pigs. Thus, the QT intervals and the activation time were calculated from the same point in this study. In addition, the local activation times from MAP recordings were found to cover the whole duration of the QRS complex in each pig.

Dispersion of ventricular repolarization

In the 10 pigs, the EOR times over the endocardium and epicardium were obtained as shown in Table 1. Three-dimensional maps of the repolarization

sequences over both the epicardium and endocardium were constructed in the 10 pigs. Of these maps, the EOR commonly started from the anteroseptal/apical area and ended in the lateral or posterolateral basal area, i.e. the minimal EOR times were all recorded around the anteroseptal/apical area, and the maximal EOR times around the lateral or posterolateral basal area (Fig. 3).

The DVR-epi, DVR-endo and DVR-total were 36±8, 51±15 and 58±11 ms, respectively. The DVR-total was significantly greater than the DVR-epi and DVR-endo ($p < 0.001$ and $p < 0.05$, respectively) (Table 1). In addition, in the 2 pigs in which both left and right ventricles were mapped, the maximal and minimal EOR times were all found in the left ventricle recordings. Thus, the measurements from the right ventricle did not affect the maximal DVR in these 2 pigs.

Dispersion parameters on surface ECG

The QT dispersion parameters are presented in Table 2. QT_{peak} dispersion was significantly smaller than QT_{end} dispersion in the 10 pigs (15±2 vs. 21±4 ms, $p < 0.01$). The minimal, mean and maximal T_{peak}-T_{end} intervals were 20±9, 44±5 and 57±7 ms, respectively. The maximal T_{peak}-T_{end} intervals were significantly greater than the minimal and mean T_{peak}-T_{end} intervals ($p < 0.0001$ and $p < 0.0001$, respectively). The maximal and mean T_{peak}-T_{end} intervals were also greater than the QT_{peak} dispersion and QT_{end} dispersion ($p < 0.0001$ vs. $p < 0.0001$). In addition, T_{peak}-T_{end} intervals from lead II and V_5 were also compared, but no significant difference was found between them (41±6 vs. 43±5 ms, $p > 0.05$). However, the T_{peak}-T_{end} intervals from both of the leads were significantly smaller than the maximal T_{peak}-T_{end} intervals ($p < 0.0001$) (Table 2).

Relationship between dispersion of ventricular repolarization and ECG dispersion parameters

No significant difference was found between the maximal T_{peak}-T_{end} interval and the DVR-total (p = 0.33), whereas the mean and minimal T_{peak}-T_{end} intervals were both significantly smaller than the DVR-total ($p < 0.01$ and $p < 0.0001$, respectively). The T_{peak}-T_{end} intervals from lead II and V_5 were also significantly smaller than the DVR-total ($p < 0.001$ and $p < 0.01$, respectively).

Correlation analyses showed that there was a high correlation between the maximal T_{peak}-T_{end} interval and the DVR-total (r = 0.64, $p < 0.05$) (Fig. 4a), whereas correlation between the mean T_{peak}-T_{end} interval and the DVR-total showed an r value of 0.56 ($p = 0.09$). The T_{peak}-T_{end} intervals from lead II and V_5 did not correlate with the DVR-total either (r = 0.30, $p = 0.40$ and r = 0.33, $p = 0.35$, respectively). In addition, no significant correlation was found when the DVR-total was compared with the QT_{peak} dispersion and QT_{end} dispersion (r = 0.07, $p = 0.84$ and r = -0.48, $p = 0.16$, respectively) (Fig. 4b and 4c).

Discussion

T_{peak}-T_{end} interval as an index of the global dispersion of ventricular repolarization

It was earlier hypothesized that the T wave vector is generated by different local levels of repolarization in the heart (21, 22), so that the T wave emerges from inhomogeneous recovery throughout the heart. Based on this theory, the T wave width, which represents the repolarization time differences in the heart, was postulated to correlate highly with the dispersion of repolarization. Thus, the T_{peak}-T_{end} interval was chosen as a measurement of half the T wave width due to the difficulties in determination of the T wave onset, and reported to be highly correlated with the dispersion of APD_{90} and recovery time in isolated rabbit heart model (23).

Recently, *in vitro* canine studies have suggested that full repolarization of the epicardium coincides with the peak of the T wave and that of the subendocardially located M cells coincides with the end of the T wave (10). The T_{peak}-T_{end} interval was therefore proposed and used as an index of transmural DVR. Several clinical studies have demonstrated the potential usefulness of this variable as a predictor of ventricular arrhythmias (24, 25). However, *in vivo* evaluation of the relationship between T_{peak}-T_{end} interval and the global DVR is still lacking.

In the present study, data from about 100 MAP recordings over both epicardium and endocardium in each of the 10 pigs were analysed using the electroanatomic mapping technique. We found that the maximal T_{peak}-T_{end} interval appeared to be similar to, and significantly positively correlated with the DVR-total. These results are not completely consistent with the previous studies (10). Since the DVR-total in this study, the maximal EOR differences over both the epicardium and endocardium, reflects not only the transmural gradients, but also the apico-basal

gradients, our results suggest that the maximal T_{peak}-T_{end} interval may be a good estimation of global DVR. To our knowledge, this is the first *in vivo* validation of the T_{peak}-T_{end} interval as an index of the global DVR. Certainly, the relationship between T_{peak}-T_{end} intervals and global DVR in this study was validated in normal heart, but not in a model of heart disease. In addition, due to the missing information on repolarization of the mid-myocardial cells, our data did not allow us to clarify the relationship between the global DVR and transmural gradients in greater depth. Further investigations are clearly needed to address these issues.

The method for T_{peak}-T_{end} interval measurement must also be established. T_{peak}-T_{end} interval measured from the earliest T_{peak} to the latest T_{end} on the 12 lead ECG, i.e. the maximal T_{peak}-T_{end} interval, may be a better index of the global DVR. As we know, time points of the T_{peak} and T_{end} vary from lead to lead, which results in the T_{peak}-T_{end} intervals showing a discrepancy on different leads of ECG. Some studies have selected special leads such as II, V_5, an average of all leads or ambulatory ECG to analyze T_{peak}-T_{end} interval (24, 26-27). However, our results have shown that the T_{peak}-T_{end} interval from lead II, V_5, or the average T_{peak}-T_{end} interval of all 12 leads did not correlate ideally with the DVR-total, but the maximal T_{peak}-T_{end} interval did. This suggests that the T_{peak}-T_{end} interval measurement from a single lead or average value from the 12 lead ECG was not reliable as an index of the global DVR. Certainly, the placement of leads in pigs in this study, especially the precordial ones, did not correspond exactly to the same leads as those in humans since the vector summation should be different due to the difference in anatomy and the changes from open-chest surgery. However, our data still demonstrate that the measurement of T_{peak}-T_{end} interval as an index of global DVR should not be obtained arbitrarily from

any lead of the surface ECG. Further explorations are clearly required in order to define the measurement of this ECG interval in humans.

QT dispersion failed to reflect global dispersion of ventricular repolarization

The measurement of QT dispersion has been proposed as a simple non-invasive measurement of DVR from 12-lead surface ECG since the 1990s (4). Increased QT dispersion was considered to reflect an increased DVR, and thereby used as a prognostic tool in detection of future malignant ventricular arrhythmias or sudden death in patients with various heart diseases (4, 5). However, numerous prognostic studies have reported contradictory results, and the interpretation of QT dispersion seems to be contradictory to the vector loop theory of ECG wave forms (7, 8).

In this study, the QT_{peak} and QT_{end} dispersion were both poorly correlated with the DVR-total, suggesting that these variables do not reflect the global DVR. This is inconsistent with previous studies (23, 28). However, the previous studies were limited by the number of MAP recordings from the ventricle. The global DVR may be poorly estimated from only a few adjacent or remote ventricular sites, as shown in a recent study (17), which may explain the inconsistency between our results and those of others. In the present study, both the epicardial and endocardial DVR were significantly smaller than the DVR-total. This result further emphasizes the importance of number of recording sites for evaluation of the global DVR. Hence, the increased QT dispersion more likely indicates a significantly disturbed T vector loop. Although this might be a risk factor of malignant ventricular arrhythmias, the QT_{peak} or QT_{end} dispersion were not reliable indexes of the global DVR.

Clinical implications

Non-invasive detection of increased DVR bears important clinical implications. The T_{peak}-T_{end} interval is easily available from 12-lead ECG and has been demonstrated in the present study to be a useful noninvasive index of the global DVR. Among the different measurement methods of this interval, the maximal T_{peak}-T_{end} interval, from the earliest T_{peak} to the latest T_{end}, was suggested by the present study to be able to be used for the estimation of the global DVR. On the other hand, based on our data, the QT_{peak} and QT_{end} dispersion were not favourable.

"Limitations of the study"

Intramural MAP recording was not available in this study. As a result, the repolarization of the mid-myocardially located M cells may be missing. However, It is not only the superficial layer of cells that is involved in the genesis of MAPs; the repolarization of deeper layer of cells could also be reflected by the MAP signals (29), although exactly how deep the MAP records and whether the M cells contribute to the genesis of the MAP is not clear. In addition, in the porcine ventricle, M cells are not only confined to the mid-myocardial layer; they are also present in the epicardial layer (30, 31). Furthermore, in contrast to man and dog, the pig has a transmural Purkinje system, so that the activation does not spread from the endocardium to the epicardium, but rather goes more or less simultaneously through the different layers of the ventricular wall (32). Importantly, the significantly longer action potential duration of M cells in isolated canine ventricle was mostly recorded at a cycle length of 2000 ms (10), whereas the transmural gradient would be markedly minimized at shorter cycle lengths, such as 130 bpm in the present study. These

factors suggest that our findings are nevertheless the most detailed *in vivo* data on global DVR available for validation of the related ECG variables.

Additionally, the MAP recordings were only performed in the left ventricle in most of the pigs, in which the repolarization of the right ventricle was missing. However, activation and repolarization in the two ventricles are synchronized and the left ventricular mass contributes predominantly to the genesis of QRS complex and the T waves. The range of local activation times on our recorded MAPs was found to cover the whole duration of the QRS complex in all the pigs, which indicates the relative completeness of our MAP mapping. Moreover, our observation in the two pigs which had both the left and right ventricles mapped showed that the minimal and maximal EOR times were located in the left ventricle in both, which further supports the validity of our data for the purpose of the current study.

Summary

Correlation analysis of the electrocardiographic parameters QT_{peak} dispersion, QT_{end} dispersion and T_{peak}-T_{end} interval with the global DVR measurements were performed in swine. The maximal T_{peak}-T_{end} interval was demonstrated to be coincident with the DVR-total, with significant positive correlation between them. However, the mean T_{peak}-T_{end} interval or T_{peak}-T_{end} intervals from a single lead were all significantly smaller than and poorly correlated with the DVR-total, as were the QT_{peak} and QT_{end} dispersion. These findings suggest that the maximal T_{peak}-T_{end} interval, but not the conventional QT dispersion parameters, could serve as a noninvasive index of the global DVR.

Acknowledgements

This study was supported by funding from the Swedish Heart-Lung Foundation, the Lund University Hospital donation funds, the Franke and Margaretha Bergqvist Foundation, and Biosense Webster/Johnson & Johnson Inc.

References

1. Kuo CS, Munakata K, Reddy CP, Surawicz B. Characteristics and possible mechanism of ventricular arrhythmia dependent on the dispersion of action potential durations. Circulation 1983; 67:1356-1367.
2. Pastore JM, Girouard SD, Laurita KR, Rosenbaum DS. Modulated dispersion explains changes in arrhythmias vulnerability during premature stimulation of the heart. Circulation 1998; 98: 2774-2780.
3. Sylven JC, Horacek BM, Spencer CA, Klassen GA, Montague TJ. QT interval variability on the body surface. J Electrocardiol 1984; 17: 179-188.
4. Day CP, McComb JM, Campbell RW. QT dispersion: an indication of arrhythmia risk in patients with long QT intervals. Br Heart J. 1990; 63:342-4.
5. Barr CS, Naas A, Freeman M, Lang CC, Struthers AD. QT dispersion and sudden unexpected death in chronic heart failure. Lancet. 1994; 343: 327-9.
6. Macfarlane PW, McLaughlin SC, Rodger C. Influence of lead selection and population on automated measurement of QT dispersion. Circulation 1998; 98: 2160-2167.
7. Lee KW, Kligfield P, Okin PM, Dower GE. Determinants of precordial QT dispersion in normal subjects. J Electrocardiol 1998; 31 Suppl: 128-133.
8. Kors JA, van Herpen G, van Bemmel JH. QT dispersion as an attribute of T-loop morphology. Circulation 1999; 99: 1458-1463.
9. Antzelevitch C, Sicouri S, Litovsky SH, Lukas A, Krishnan SC, Di Diego JM, Gintant GA, Liu DW. Heterogeneity within the ventricular wall: electrophysiology and pharmacology of epicardial, endocardial and M cells. Cir Res 1991; 69: 1427-1449.

10. Yan GX, Antzelevitch C. Cellular basis for the normal T wave and the electrocardiographic manifestations of the long QT syndrome. Circulation 1998; 98: 1928-1936.
11. Lubinski A, Kornacewicz-Jach Z, Wnuk-Wojnar AM, Adamus J, Kempa M, Krolak T, Lewicka-Nowak E, Radomski M, Swiatecka G. The terminal portion of T wave: A new electrocardiographic marker of risk of ventricular arrhythmias. Pacing Clin Electrophysiol 2000; 23: 1957-1959.
12. Taggart P, Sutton PM, Opthof T, Coronel R, Trimlett R, Pugsley W, Kallis P. Transmural repolarisation in the left ventricle in humans during normoxia and ischaemia. Cardiovasc Res. 2001; 50(3): 454-62.
13. Smetana P, Pueyo E, Hnatkova K, Batchvarov V, Camm AJ, Malik M. Effect of Amiodarone on the Descending Limb of the T Wave. Am J Cardiol 2003; 92:742–746.
14. Yuan S, Blomstrom-Lundqvist C, Olsson SB. Monophasic action potentials: concepts to practical applications. J Cardiovasc Electrophysiol. 1994; 5: 287-308.
15. Franz MR. Current status of monophasic action potential recording: theories, measurements and interpretations. Cardiovasc Res. 1999; 41: 25-40.
16. Yuan S, Kongstad O, Hertervig E, Holm M, Grins E, Olsson B. Global repolarization sequence of the ventricular endocardium: monophasic action potential mapping in swine and humans. Pacing Clin Electrophysiol 2001; 24: 1479-1488.
17. Kongstad O, Yuan S, Hertervig E, Holm M, Grins E, Olsson B. Global and local dispersion of ventricular repolarization: endocardial monophasic action

potential mapping in swine and humans by using an electro-anatomical mapping system. J Electrocardiol. 2002; 35:159-67.

18. Xia Y, Kongstad O, Hertervig E, Li Z, Holm M, Olsson B, Yuan S. Activation recovery time measurements in evaluation of global sequence and dispersion of ventricular repolarization. J Electrocardiol. 2005; 38(1):28-35.
19. Gepstein L, Hayam G, Ben-Haim SA. A novel method for nonfluoroscopic catheter-based electroanatomical mapping of the heart. In vitro and in vivo accuracy results. *Circulation* 1997; 95: 1611-1622.
20. Liu S, Yuan S, Hertervig E, Kongstad O, Holm M, Grins E, Olsson SB. Monophasic action potential mapping in swine and humans using modified-tip ablation catheter and electroanatomic mapping system. Scand Cardiovasc J. 2002;36(3):161-6.
21. Harumi K, Burgess MJ, Abildskov JA. A theoretic model of the T wave. Circulation 1966; 34: 657-668.
22. Franz MR, Bargheer K, Costard-Jackle A, Miller DC, Lichtlen PR. Human ventricular repolarization and T wave genesis. Prog Cardiovasc Dis 1991; 33: 369-384.
23. Zabel M, Portnoy S, Franz MR. Electrocardiographic indexes of dispersion of ventricular repolarization: an isolated heart validation study. J Am Coll Cardiol. 1995; 25: 746-52.
24. Lubinski A, Lewicka-Nowak E, Kempa M, Baczynska AM, Romanowska I, Swiatecka G. New insight into repolarization abnormalities in patients with congenital long QT syndrome: the increased transmural dispersion of repolarization. PACE 1998; 21:172-175.

25. Medina-Ravell VA, Lankipalli RS, Yan GX, Antzelevitch C, Medina-Malpica NA, Medina-Malpica OA, Droogan C, Kowey PR. Effect of Epicardial or Biventricular Pacing to Prolong QT Interval and Increase Transmural Dispersion of Repolarization: Does Resynchronization Therapy Pose a Risk for Patients Predisposed to Long QT or Torsade de Pointes? Circulation. 2003; 107: 740-746.
26. Davey PP. QT interval measurement: Q to TApex or Q to TEnd? Journal of Internal Medicine 1999; 246: 145-149.
27. Nakagawa M, Takahashi N, Watanabe M, Ichinose M, Nobe S, Yonemochi H, Ito M, Saikawa T. Gender differences in ventricular repolarization: terminal T wave interval was shorter in women than in men. Pacing Clin Electrophysiol 2003; 26: 59-64.
28. Zabel M, Lichtlen PR, Haverich A, Franz MR. Comparison of ECG variables of dispersion of ventricular repolarization with direct myocardial repolarization measurements in the human heart. J Cardiovasc Electrophysiol 1998; 9: 1279-1284.
29. Knollmann BC, Tranquillo J, Sirenko SG, Henriquez C, Franz MR. Microelectrode Study of the Genesis of the Monophasic Action Potential by Contact Electrode Technique. J Cardiovasc Electrophysiol, 2002, 13, 1246-1252.
30. Stankovicova T, Szilard M, De Scheerder I, Sipido KR. M cells and transmural heterogeneity of action potential configuration in myocytes from the left ventricular wall of the pig heart. Cardiovasc Res. 2000; 45(4): 952-60.

31. Yan GX, Shimizu W, Antzelevitch C. The characteristics and distribution of M cells in arterially-perfused canine left ventricular wedge preparations. Circulation 1998; 98: 1921-1927.
32. Hamlin RL, Burton RR, Leverett SD, Burns JW. Ventricular activation process in minipigs. J Electrocardiol. 1975;8(2): 113-6.

Table 1: The end of repolarization time and its dispersion over epicardium and endocardium during right atrial pacing 130 bpm in 10 pigs

Pigs	Epicardium of LV			Endocardium of LV			DVR-total
	Sites	EOR	DVR	Sites	EOR	DVR	
1	67	313±10	39	56	322±14	63	63
2	67	311±10	39	59	313±19	77	77
3	32	328±6	29	57	353±15	61	67
4	49	272±7	26	75	281±12	55	55
5	47	323±11	48	72	315±9	32	50
6	50	299±8	31	49	295±15	64	64
7	47	294±7	27	66	302±8	32	38
8	45	340±11	45	59	352±11	43	63
9	48	282±8	38	77	303±10	40	52
10	57	303±9	33	70	315±12	46	53
Total	51±10	306±21	36±8*	64±9	312±25	51±15†	58±11

Data of EOR are presented as mean ± 1 standard deviation in milliseconds. EOR: end of repolarization time; LV: left ventricle; DVR: dispersion of ventricular repolarization. * $p < 0.001$ and † $p < 0.05$ compared with the DVR-total.

Table 2: ECG dispersion parameters in the 10 pigs

Pigs	Min T_p-T_e	Mean T_p-T_e	Max T_p-T_e	T_p-T_e V_5	T_p-T_e II	QT_p Disp	QT_e Disp
1	33	48	66	48	49	14	19
2	18	44	56	44	37	15	23
3	33	47	60	44	46	12	15
4	19	44	57	44	41	17	21
5	16	40	49	43	49	11	22
6	30	48	64	51	46	18	16
7	4	41	48	43	34	15	29
8	19	41	55	39	40	14	22
9	18	36	46	37	34	12	16
10	14	40	54	35	37	17	23
Total	20±9	*44±5	57±7	*43±5	*41±6	15±2	†21±4

Total are data from the 10 pigs as mean ± 1 standard deviation in milliseconds. Min, Mean and Max T_p-T_e: minimal and maximal T_{peak} to T_{end} interval. II and V_5: Lead II and V_5. QT_p and QT_e Disp: QT_{peak} and QT_{end} dispersion, respectively. * $p < 0.0001$ compared with Max T_p-T_e. † $p < 0.01$ compared with QT_p Disp.

Legends

Fig. 1: Selected monophasic action potential recordings from the 2-d views of all the MAPs from the epicardium (left) and endocardium (right) in Pig no. 10. Recording sites over both epicardium (n = 57) and endocardium (n = 70) are displayed.

Fig. 2. One of the 6 ECG measurements from pig no. 8. In each ECG lead, the first vertical line denotes the earliest activation time, and the second vertical line denotes the end of the T wave. The short white line marks the peak of the T wave. The values on the second line in each lead are QT_{end} intervals, and the maximal T_{peak}-T_{end} interval on this measurement occasion is 52 milliseconds.

Fig. 3: CARTO maps of the end of repolarization sequences of the epi- (left) and endocardium (right) from pig 6. The end of repolarization (EOR) started from the apical area and ended in the posterolateral basal area. The minimal recorded EOR time is 264 ms, and the maximal recorded EOR time is 328 ms.

Fig. 4: Correlation analysis between the maximal T_{peak}-T_{end} interval and the global dispersion of ventricular repolarization of all recordings (DVR-total), QT_{peak} dispersion and the DVR-total, as well as QT_{end} dispersion and the DVR-total. The maximal T_{peak}-T_{end} interval is highly correlated with the DVR-total (Fig.4a), whereas the QT_{peak} dispersion and QT_{end} dispersion correlates poorly with the DVR-total (Fig. 4b and 4c).

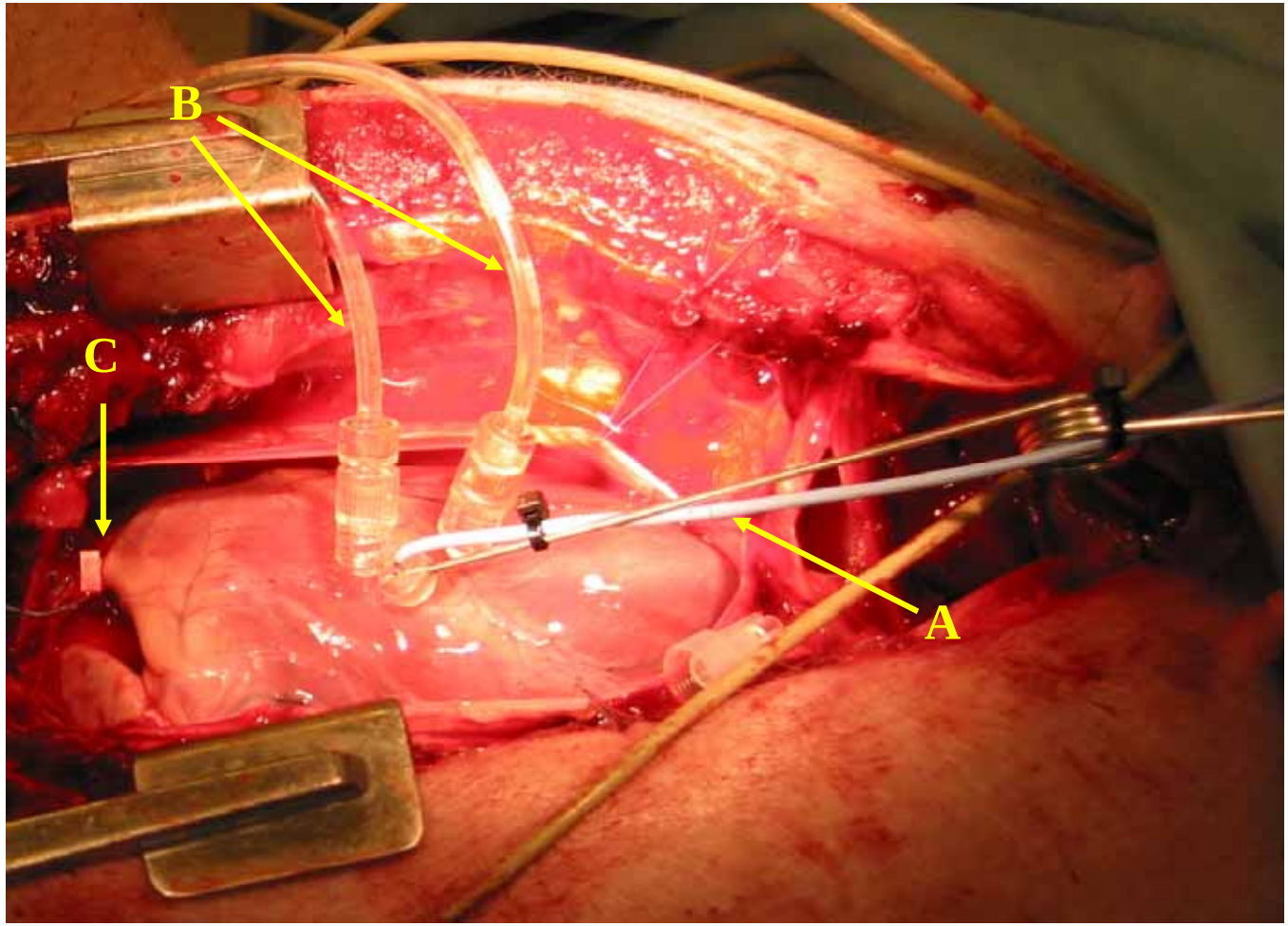

Fig. 1

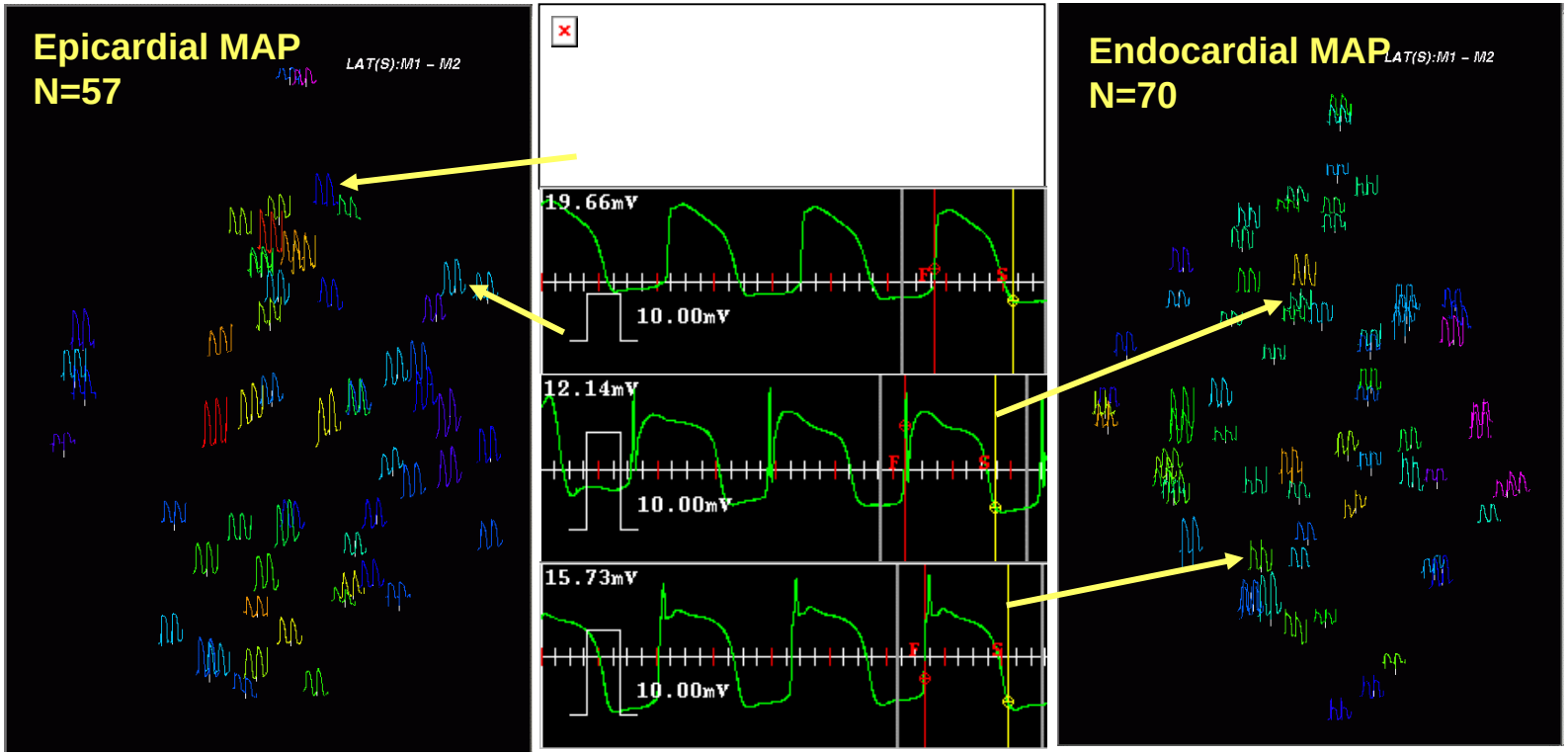
Epicardial MAP
N=57
LAT(S):M1 – M2
19.66mV
10.00mV
12.14mV
10.00mV
15.73mV
10.00mV
Endocardial MAP
LAT(S):M1 – M2
N=70

Fig. 2

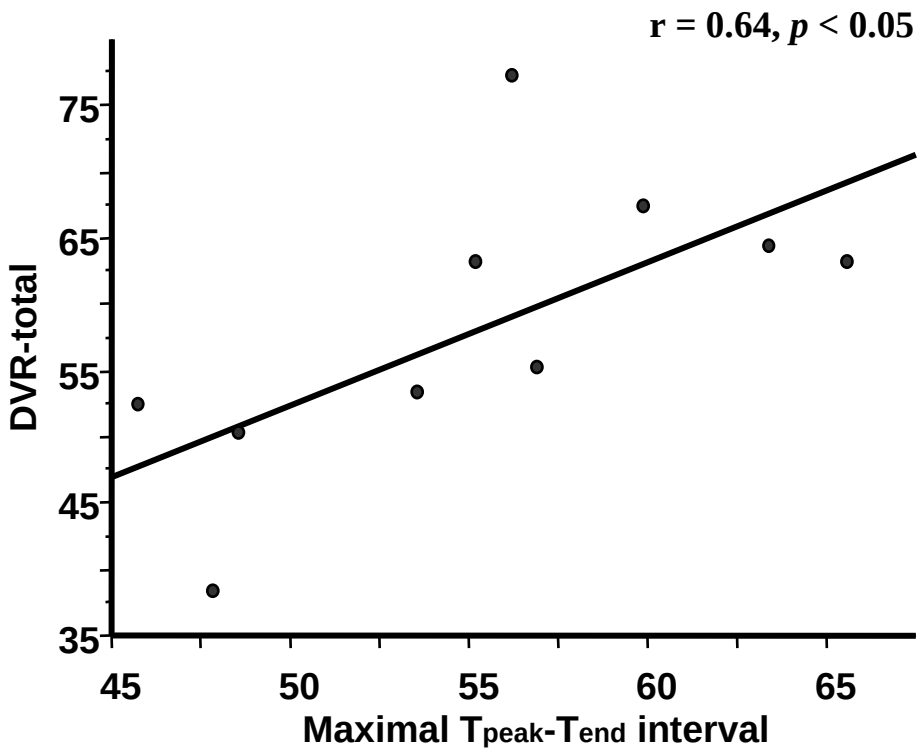
r = 0.64, p < 0.05
DVR-total
75
65
55
45
35
45
50
55
60
65
Maximal Tpeak-Tend interval

a

Fig. 4

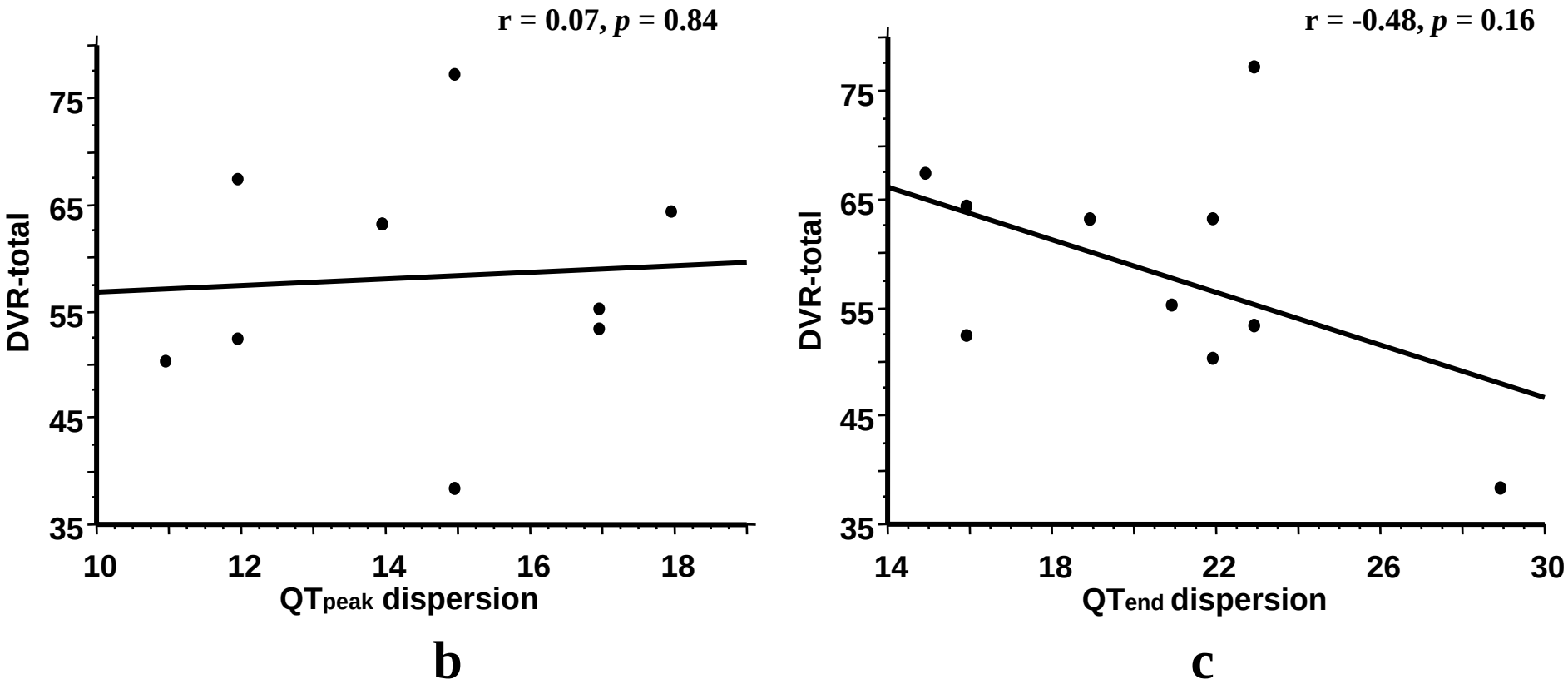
r = 0.07, p = 0.84
DVR-total
75
65
55
45
35
10
12
14
16
18
QTpeak dispersion
b
r = -0.48, p = 0.16
DVR-total
75
65
55
45
35
14
18
22
26
30
QTend dispersion
c

Fig. 4

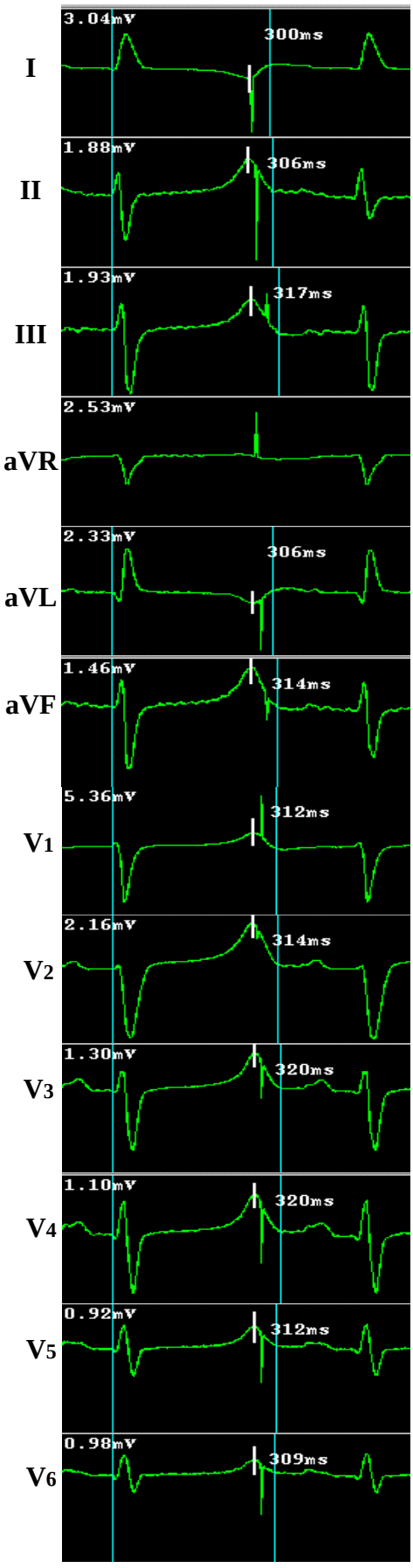
I
3.04mV
300ms
II
1.88mV
306ms
III
1.93mV
317ms
aVR
2.53mV
aVL
2.33mV
306ms
aVF
1.46mV
314ms
V1
5.36mV
312ms
V2
2.16mV
314ms
V3
1.30mV
320ms
V4
1.10mV
320ms
V5
0.92mV
312ms
V6
0.98mV
309ms

Fig. 3